4-Thiazolidinone derivatives as MMP inhibitors in tissue damage: synthesis, biological evaluation and docking studies

Matteo Incerti[1], Lucia Crascì[2,*], Paola Vicini[1], Esin Aki[3], Ismail Yalcin[3], Tugba Ertan-Bolelli [3], Venera Cardile[4], Adriana Graziano[4] and Annamaria Panico[2].

[1] Department of Food and Drug, University of Parma, Parco Area delle Scienze 27/A, 43124 Parma, Italy, matteo.incerti@unipr.it, paola.vicini@unipr.it

[2] Department of Drug Sciences, University of Catania, V. le A. Doria 6, 95125 Catania, Italy, panico@unict.it

[3] Pharmaceutical Chemistry Department, Faculty of Pharmacy, Ankara University, 06100 Tandogan, ANKARA, esinaki@ankara.edu.tr, yalcin@ankara.edu.tr, tbolelli@ankara.edu.tr

[4] Department of Physiological Sciences, University of Catania, V. le A. Doria 6, 95125 Catania, Italy, cardile@unict.it, acegraziano@tiscali.it.

*Corresponding author:
Dr Lucia Crascì
luciacrasci@alice.it
+39 0957384012/4013

Abstract

Nine 2-(1,2-benzothiazol-3-yl)-N-(4-oxo-2-phenyl-1,3-thiazolidin-3-yl) propanamides were designed and synthesized, combining benzisothiazole and 4-thiazolidinone in one frame. The aim of the study was to verify their effectiveness to contrast the inflammatory/oxidative process in which free oxygen and nitrite (ROS and RNS) radicals, advanced glycation products (AGEs), inflammatory cytokines and matrix metalloproteinases (MMPs) are involved. Docking studies of all the compounds were performed in order to explore their binding mode at the MMP-9 protein. An appreciable anti-inflammatory/wound healing effects of the tested compounds was highlighted. Derivative **23**, bearing a 4-carboxyphenyl substituent at C2 of the 4-thiazolidinone ring, exhibited the highest activity, being able to inhibit MMP-9 at nanomolar level (IC_{50} = 40 nM).

Keywords: 4-Thiazolidinones; ORAC assay; Metalloproteinase-9; Docking study; Keratinocytes cultures; Nuclear factor -kB.

Preprints (www.preprints.org) | NOT PEER-REVIEWED | Posted: 31 October 2017 doi:10.20944/preprints201710.0200.v1

Peer-reviewed version available at Molecules 2018, 23, 415; doi:10.3390/molecules23020415

1. Introduction

Chronic inflammation causes tissue damage and has been identified as contributing to a host of diseases including cardiovascular, pulmonary, neurodegenerative, metabolic/obesity-related diseases [1]. All diseases in which the inflammatory process becomes destructive to the tissues activated repeatedly or inappropriately from free oxygen and nitrite (ROS and RNS) radicals, advanced glycation products (AGEs), inflammatory cytokines and matrix metalloproteinases (MMPs). Moreover, it is well established that accumulation of oxygen free radicals (ROS) and advance glycation products (AGEs), can activate a cascade of radical reactions, causing the up-regulation of MMPs production, *via* activation of eukaryotic nuclear factor κB (NF-κB) pathway [2]. NF-κB is a transcription factor that is a regulator of immune responses stimulated by pro-inflammatory agents such as interleukin-1β (IL-1β) and tumor necrosis factor α (TNF-α), and is sensitive to cellular redox modifications. [3]. ROS appears to be responsible for IL-1β-induced NF-kB activation and inducible nitric oxide synthase (iNOS) expression [4]. RNS, as nitric oxide (NO) and peroxynitrite, in turn, exert proinflammatory and catabolic effects, by providing a persistent activation of NF-kB and, consequently, NF-kB-dependent transcription of MMPs (Figure 1) [2].

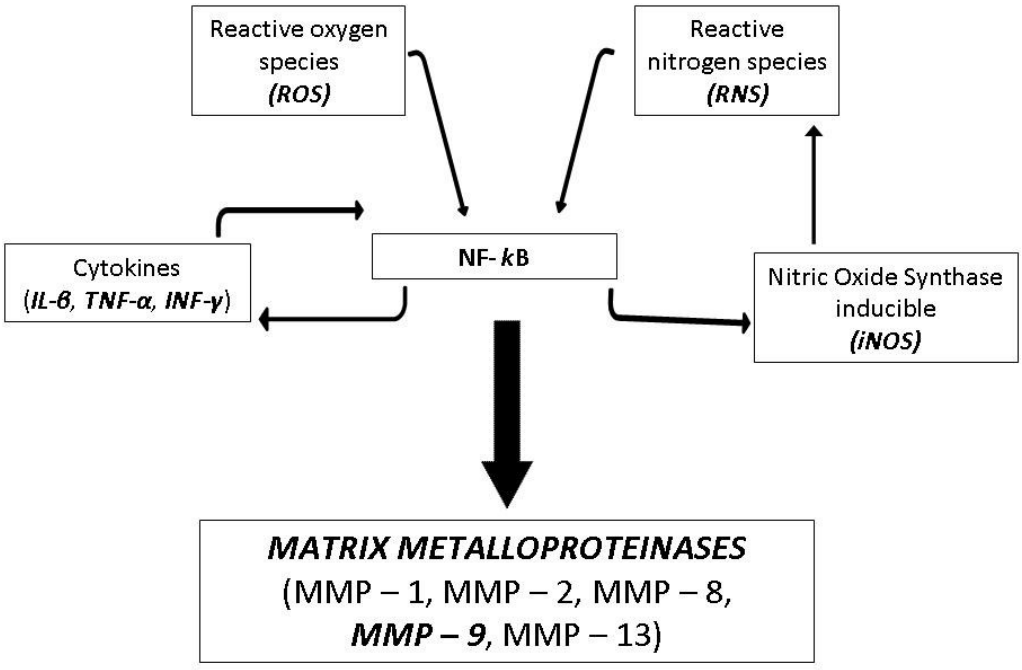

Figure 1. MMPs activation *via* oxygen and nitrite (ROS and RNS) radicals, pro-inflammatory cytokines and growth factors) and inducible nitric oxide synthase (iNOS).

An increased levels of MMPs, as elastase, plasmin and thrombin, destroy components of the extracellular matrix (ECM), causing chronic inflammation and tissue damage.

The tissue integrity is a complex biological process and ECM participates actively to stabilization of tissue structure. The ECM is composed of a variety of polysaccharides, water and collagen proteins which give the skin remarkable properties. In tissue damage (vascular endothelium), increased levels of proteases such as MMPs, important components in many biological and pathological processes, destroy components of the ECM, and epithelial-derived MMP-9 is an important mediator of tissue injury [5].

The MMPs are part of a large family of enzymatic calcium-dependent endopeptidase containing zinc ions. They are produced mainly by connective tissue cells and are responsible, by means of catalysis of the hydrolysis of peptide bonds at the level of specific amino acid sequences, of tissue remodeling and degradation of great majority of the ECM components (collagen, elastin, gelatin, matrix of glycoproteins and peptidoglycans).

The use of selective inhibitors specific for metalloproteases may lead to monitoring and improvement of these diseases. However, the problem in search is the selectivty. Most of MMPs retains common structural features, such as the presence of a catalytic zinc ion and many equalities in the amino acid sequences in the binding site [6].

Most of the MMPs inhibitors reported in the literature possess a functional group able to chelate the catalytic zinc present in the active site of the enzyme, the Zinc-Binding-Group (ZBG), and a planar and lipophilic portion able to mainly occupy the binding site S1'. Derivatives with hydroxamic function result potent and effective inhibitors [7]. However, they show toxicity and poor bioavailability prompting the search for new molecules with greater efficacy and selectivity.

The objective of this work was the design of novel 4-thiazolidinone derivates as MMP inhibitors in tissue damage. Nine 2-(1,2-benzothiazol-3-yl)-N-(4-oxo-2-phenyl-1,3-thiazolidin-3-yl)propanamides were designed and synthesized. The designed compounds combine two bioactive moieties: benzisothiazole and 4-thiazolidinone in one frame. We planned to introduce also an isopropanoylhydrazide spacer, between the two heterocycles, aimed at emphasizing their antinflammatory/protective effects on keratinocytes. All of the novel 4-thiazolidinone derivates bear an aromatic moiety at C2 of the 4-thiazolidinone ring with hydrophobic/ hydrophilic/hydrogen-donor group at C4 to evaluate their importance for activity. Furthermore, docking studies of all of the compounds were performed in order to explore the binding mode at the MMP-9 protein, helping us to gain understanding of the

pharmacophoric requirements necessary for the activity and for the rational design of new inhibitors.

2. Results and discussion

2.1. Chemistry

The target compounds **13**-**19**, **22** and **23** were synthesized using a stepwise reaction protocol (Scheme 1), starting from 2-(1,2-benzothiazol-3-yl)propanoic acid (**1**), synthesized using procedures reported earlier [8] starting from 3-chloro-1,2-benzothiazole. Heating **1** and ethanol in the presence of concentrated sulfuric acid gave 2-(1,2-benzothiazol-3-yl)propanoic acid ethyl ester **2**. By reacting this ethyl ester and hydrazine-hydrate in methanol 2-(1,2-benzothiazol-3-yl)propanoic acid hydrazide **3** was obtained [9]. Hydrazide **3** was allowed to react with commercially available aldehydes or with 4-formylphenyl acetate (FPA) [10] and methyl 4-formylbenzoate (MFB) [11], in turn obtained through reaction from commercially available aldehydes. FPA and MFB were prepared to convert the hydroxyl and carboxyl group of 4-hydroxy- and 4-carboxybenzhaldeyde in their ester derivatives with the purpose to avoid decomposition that occurred without protection in the final cyclocondesation step. Refluxing an ethanolic solution of **3** with the proper aldehydes in the presence of acetic acid led to 2-(1,2-benzothiazol-3-yl)-*N*'-phenylmethylidene)propanehydrazides **4**-**12**. Reaction (cyclocondesation) of the hydrazides **4-12** with sulfanylacetic acid in refluxing toluene, in N_2 atmosphere, afforded 2-(1,2-benzothiazol-3-yl)-*N*-(4-oxo-2-phenyl-1,3-thiazolidin-3-yl)propanamides **13-21** in good yield. Finally, deprotection of **20** and **21** under basic conditions, led to the formation of the target derivatives **22** and **23**.

Preprints (www.preprints.org) | NOT PEER-REVIEWED | Posted: 31 October 2017 doi:10.20944/preprints201710.0200.v1

Peer-reviewed version available at Molecules 2018, 23, 415; doi:10.3390/molecules23020415

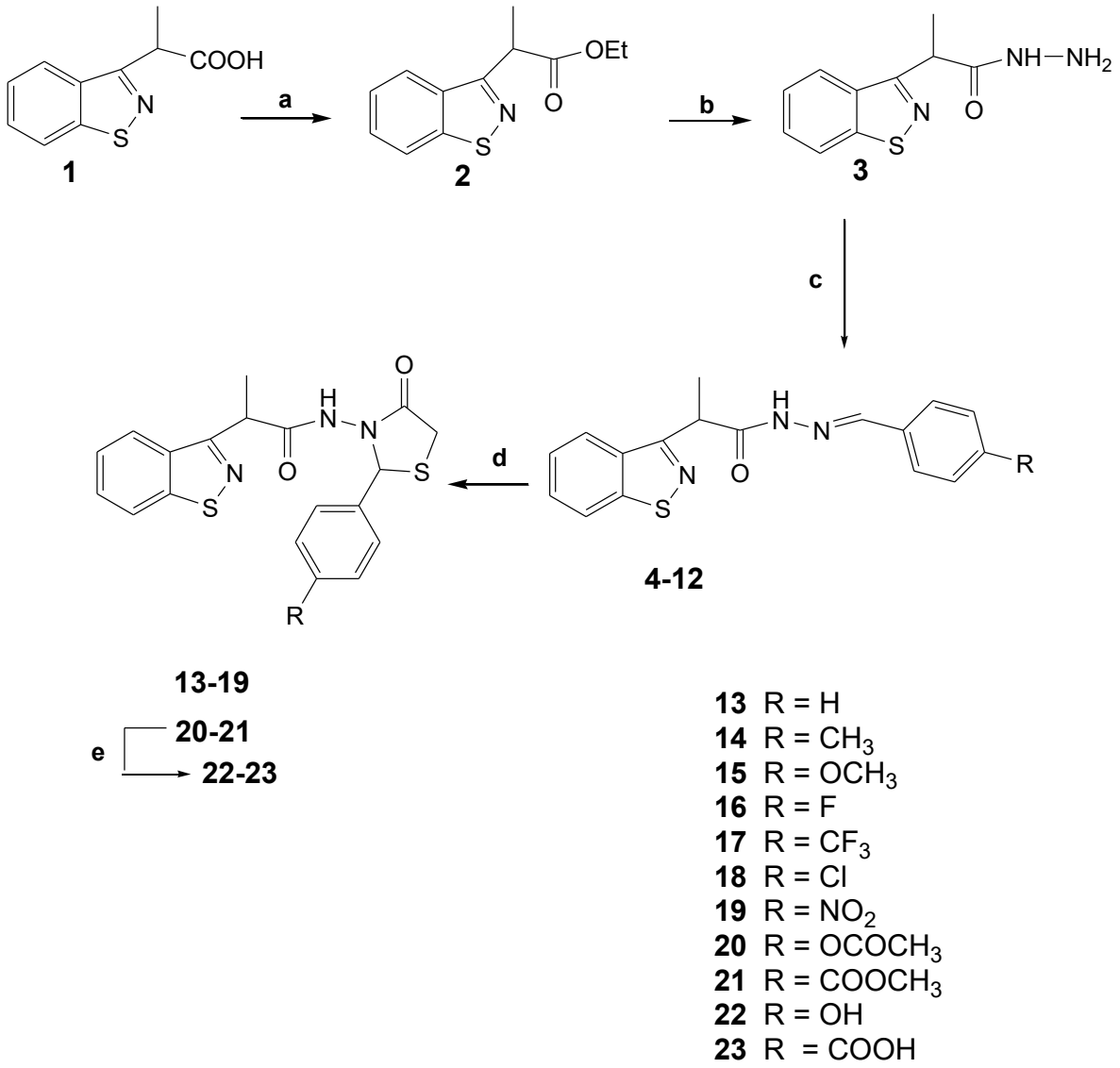

Scheme 1. Reagents and conditions: (a) conc. H_2SO_4, EtOH, reflux, 8 h; (b) NH_2NH_2, MeOH, rt, 2 h; (c) R-C_6H_4CHO, CH_3COOH, EtOH, reflux, 8 h or MFB or FPA, CH_3COOH, EtOH, reflux, 5 h; (d) $HSCH_2COOH$, $CH_3C_6H_5$, reflux, 48 h; (e) NaOH, EtOH, rt, 2 h; then HCl.

2.2. Synthesis

Unless otherwise noted, reagents were obtained from commercial suppliers and were used without purification. Anhydrous toluene was obtained by distillation from Na, and anhydrous CH_2Cl_2 was obtained by distillation from calcium hydride. Melting points were measured on a Buechi 512 apparatus (Buechi Italia, Milano, Italia) and are uncorrected. The progress of the reactions was monitored by TLC with F254 silica-gel precoated sheets (Merck, Darmstadt, Germany). UV light was used for detection. Flash chromatography was performed using Merck silica gel 60 (Si 60, 40–63 ìm, 230–400 mesh ASTM). Elemental analyses for C, H, and N were performed using a ThermoQuest Flash 1112 elemental analyzer (Termoquest Italia, Milano, Italy). The percentages found were within ± 0.4% of

the theoretical values. IR spectra were recorded on a Jasco FT-IR 460 plus spectrometer (Jasco Europe, Carpi (MO, Italia). ^{1}H-NMR spectra were recorded on a Bruker Avance 400 spectrometer (Bruker Italia, Milano, Italia). Spectra were acquired from samples in DMSO-d_6. Chemical shifts are reported as δ (ppm) relative to tetramethylsilane; coupling constants (*J*) are expressed in Hz.

General procedure for the synthesis of 2-(1,2-benzothiazol-3-yl)-N'-(phenylmethylidene) propanehydrazides 4-12

The solution (or suspension for **11** and **12**) of 2-(1,2-benzothiazol-3-yl)propanoic acid hydrazide (1,35 mmol) and the suitable aldehyde (1,38 mmol) in 15 ml anhydrous ethanol, was refluxed for 8 hours in the presence of acetic acid (0,25 ml). The mixture was cooled to room temperature, and the precipitate formed was filtered off, washed with water and then recrystallized from ethanol-water.

***2-(1,2-Benzothiazol-3-yl)-N'-(phenylmethylidene)propanehydrazide* (4)**

Mp: 179-180 °C, yield 94%. TLC; CH_2Cl_2/EtOH, 95:5. FTIR (KBr, *v*, cm^{-1}): 3183 (NH), 3003-2932 (CH3), 1670 (C=O), 1648 (CH=N). ^{1}H NMR (DMSO-d_6, *δ*, ppm): 11,45 (s, 1H, NH); 8,27-8,22 (m, 2H, Ar4+ Ar7); 7,84 (s, 1H, CH); 7,65-7,56 (m, 2H, Ar5+ Ar6); 7,22-7,18 (m, 4H, Ar2'+6'+3'+5'); 5,22 (q, 1H, *J*=7,2, CH); 1,54 (d, 1H, *J*=7,2, CH_3).

***2-(1,2-Benzothiazol-3-yl)-N'-[(4-methylphenyl)methylidene]propanehydrazide* (5)**

Mp: 173-174 °C, yield 96%. TLC; CH_2Cl_2/EtOH, 95:5. FTIR (KBr, *v*, cm^{-1}): 3201 (NH), 3049-2983 (CH_3), 1659 (C=O), 1547 (CH=N). ^{1}H NMR (DMSO-d_6, *δ*, ppm): 11,43 (s, 1H, NH); 8,27-8,16 (m, 2H, Ar4+Ar7); 7,80 (s, 1H, CH); 7,64-7,56 (m, 2H, Ar5+Ar6); 7,08 (d, 2H, *J*=7,2, Ar2'+6'); 7,00 (d, 2H, *J*=7,6, Ar3'+Ar5'); 5,19 (q, 1H, *J*=7,2 CH); 2,24 (s, 3H, CH_3); 1,52 (d, 3H, *J*=6,8).

***2-(1,2-Benzothiazol-3-yl)-N'-[(4-methoxyphenyl)methylidene]propanehydrazide* (6)**

Mp: 198-199 °C, yield 83%. TLC; CH_2Cl_2/EtOH, 95:5. FTIR (KBr, *v*, cm^{-1}): 3201 (NH), 3059-2858 (CH_3), 1663 (C=O), 1605 (CH=N). ^{1}H NMR (DMSO-d_6, *δ*, ppm): 11,32 (s, 1H, NH); 8,26-8,16 (m, 2H, Ar4+Ar7); 7,80 (s, 1H, CH); 7,65-7,51 (m, 2H, Ar5+Ar6); 7,18 (d, 2H, *J*=8,4 Ar3'+Ar5'); 6,77 (d, 2H, *J*=8,8 Ar2'+Ar6'); 5,19 (q, 1H, *J*=7,2 CH); 3,74 (s, 3H, CH_3O); 1,53 (d, 3H, *J* =6,8 CH_3).

***2-(1,2-Benzothiazol-3-yl)-N'-[(4-fluorophenyl)methylidene]propanehydrazide* (7)**

Mp: 184-185 °C, yield 89%. TLC; CH_2Cl_2/EtOH, 95:5. FTIR (KBr, *v*, cm^{-1}): 3185 (NH), 3043-2980 (CH_3), 1661 (C=O), 1602 (CH=N). ^{1}H NMR (DMSO-d_6, δ, ppm): 11,48 (s, 1H, NH); 8,26-8,16 (m, 2H, Ar4+Ar7); 7,84 (s, 1H, CH); 7,66-7,51 (m, 2H, Ar5+Ar7); 7,30-7,26 (m, 2H, Ar2'+6'); 7,06-7,02 (m, 2H, Ar3'+5'); 5,20 (q, 1H, *J*=6,8 CH); 1,54 (d, 3H, *J*=6,8 CH_3).

***2-(1,2-Benzothiazol-3-yl)-N'-{[4-trifluoromethyl)phenyl]methylidene}propanehydrazide* (8)**

Mp: 173-175 °C, yield 73%. TLC; CH_2Cl_2/EtOH, 95:5. FTIR (KBr, *v*, cm^{-1}): 3208 (NH), 2986-2890 (CH_3), 1705 (C=O), 1605 (CH=N). ^{1}H NMR (DMSO-d_6, δ, ppm): 11,74 (s, 1H, NH); 8,29-8,16 (m, 2H, Ar4+Ar7); 7,90 (s,1H, CH); 7,67-7,52 (m, 2H, Ar5+Ar7); 7,52 (d, 2H, *J*=8,0 Ar3'+5'); 7,40 (d, 2H, *J*=8,4 Ar2'+6'); 5,22 (q, 1H, *J*=7,2 CH); 1,54 (d, 3H, *J*=7,3 CH_3).

***2-(1,2-Benzothiazol-3-yl)-N'-[(4-chlorophenyl)methylidene]propanehydrazide* (9)**

Mp: 238-240 °C, yield 77%. TLC; CH_2Cl_2/EtOH, 95:5. FTIR (KBr, *v*, cm^{-1}): 3148 (NH), 2982-2933 (CH_3), 1698 (C=O), 1613 (CH=N). ^{1}H NMR (DMSO-d_6, δ, ppm): 11,51 (S, 1H, NH); 8,22-8,16 (m, 2H, Ar4+Ar7); 7,82 (s, 1H, CH); 7,60-7,49 (m, 2H, Ar6+Ar5); 7,26-7,20 (m, 4H, Ar2'+3'+5'+6'); 5,20 (q, 1H, *J*=7,2 CH); 1,53 (d, 3H, *J*=7,2 CH_3).

***2-(1,2-Benzothiazol-3-yl)-N'-[(4-nitrophenyl)methylidene]propanehydrazide* (10)**

Mp: 178-179 °C, yield 72%. TLC; EtOAc/Hex, 4:6. FTIR (KBr, *v*, cm^{-1}): 3145 (NH), 2974-2932 (CH_3), 1698 (C=O), 1513 (CH=N). ^{1}H NMR (DMSO-d_6, δ, ppm): 11,76 (s, 1H, NH); 8,30-8,27 (m, 2H, Ar4+Ar7); 8,01 (d, 2H, *J*=8,8, Ar3'+5'); 7,93 (s, 1H, CH); 7,68-7,59 (m, 2H, Ar5+ Ar6); 7,42 (d, 2H, *J*=8,8, Ar2'+6'); 5,24(q, 1H, *J*=7,0 CH); 1,55 (d, 3H, *J*=7,2 CH_3).

***4-[{2-[2-(1,2-Benzothiazol-3-yl)propanoyl]hydrazinylidene}methyl]phenyl acetate* (11)**

Mp: 168-170 °C, yield 88%. TLC; CH_2Cl_2/EtOH, 95:5. FTIR (KBr, *v*, cm^{-1}): 3184 (NH), 3010-2980 (CH_3), 1766 (C=O), 1670 (C=O), 1647 (CH=N). ^{1}H NMR (DMSO-d_6, δ, ppm): 11,47 (s, 1H, NH); 8,28-8,16 (m, 2H, Ar4+Ar7); 7,84 (s, 1H, CH); 7,66-7,50 (m, 2H, Ar5+Ar6); 7,23 (d, 2H, *J*=8,4 Ar3'+Ar5'); 6,95 (d, 2H, *J*=8,4 Ar2'+6'); 5,20 (q, 1H, *J*=7,0, CH); 2,25 (s, 3H, CO CH_3); 1,53 (d, 3H, *J*=7,2 CH_3).

***Methyl 4-[{2-[2-(1,2-benzothiazol-3-yl)propanoyl]hydrazinylidene}methyl]benzoate* (12)**

Mp: 197-199°C, yield 88%. TLC; CH_2Cl_2/EtOH, 95:5. FTIR (KBr, *v*, cm^{-1}): 3246 (NH), 2987-2945 (CH_3), 1697 (C=O), 1594 (CH=N). ^1H NMR (DMSO-d_6, *ä*, ppm): 11,63 (s, 1H, NH); 8,24-8,17 (dm, CH, Ar4+Ar7); 7,88 (s, 1H, CH); 7,72 (d, 2H, *J*=8,4 Ar3'+5'); 7,684-7,583 (m, 2H, Ar5+Ar6); 7,28(d, 2H, *J*=8,4); 5,21 (q, 1H, *J*=6,8 CH); 3,83 (s, 3H, CH_3); 1,53 (d, 3H, *J*=7,2 CH_3).

General procedure for the synthesis of 2-(1,2-benzothiazol-3-yl)-N-(4-oxo-2-phenyl-1,3-thiazolidin-3-yl)propanamides 13-19

A mixture of appropriate hydrazides **4-10** (1,1 mmol) and sulfanylacetic acid (2,2 mmol) was refluxed for 48 hours in 20 ml dry toluene, under a nitrogen atmosphere. The reaction mixture was then cooled to room temperature and the solid precipitated was filtered off and washed with toluene (or filtered, after the mixture was concentrated in vacuo (**19**), and then taken up with an aqueous solution of 10 % Na_2CO_3 and washed with water, as for **18**). The crude product was then purified by flash chromatography and recrystallized or directly recrystallized.

***2-(1,2-Benzothiazol-3-yl)-N-(4-oxo-2-phenyl-1,3-thiazolidin-3-yl)propanamide* (13)**

Mp: 239-240°C (EtOH-H_2O), yield 44%. TLC; EtOAc/Hex, 4:6. FTIR (KBr, *v*, cm^{-1}): 3221 (NH), 3036-2938 (CH_3), 1714 (C=O), 1663 (CH=N). ^1H NMR (DMSO-d_6, *δ*, ppm): 10,68 (s, 1H, NH); 8,15 (d, 1H, *J*=8,0 Ar4); 7,69 (d, 1H, *J*=8,4 Ar7); 7,57 (t, 1H, *J*=7,8 Ar5); 7,39-7,32 (m, 5H, Ar2'+3'+4'+5'+6'); 7,25 (t, 1H, *J*=7,4 Ar6); 5,17 (s, 1H, CH); 4,27 (q, 1H, *J*=6,9 CH); 3,89 (d, 1H, *J*=16,0 CH-H); 3,75 (d, 1H, *J*=15,6 CH-H); 1;55 (d, 1H, *J*=6,8 CH_3).

***2-(1,2-Benzothiazol-3-yl)-N-[2-(4-methylphenyl)-4-oxo-1,3-thiazolidin-3-yl]propanamide* (14)**

Flash chromatography; CH_2Cl_2/MeOH(NH_3), 98:2. Mp: 218-220°C (Toluene-EtOH), yield 65%. TLC; EtOAc/Hex, 4:6. FTIR (KBr, *v*, cm^{-1}): 3244 (NH), 3031-2983 (CH_3), 1713 (C=O), 1669 (CH=N). ^1H NMR (DMSO- d_6, *δ*, ppm): 10,64 (s, 1H, NH); 8,16 (d, 1H, *J*=8,4 Ar4); 7,70 (d, 1H, *J*=8,0 Ar7); 7,58 (t, 1H, *J*=7,2 Ar5); 7,33-7,14 (m, 5H, Ar6+Ar2'+6'+3'+5'); 5,71 (s, 1H, CH); 4,26 (q, 1H, *J*=6,8 CH); 3, 64 (`, 1H, *J*=16,0 BH-H); 3,74 (d, 1H, *J*=15,60 CH-H)» 2,33 (r, 3H, CH_3); 1,54 (d, 3H, *J*=7,2 CH_3).

2-(1,2-Benzothiazol-3-yl)-N-[2-(4-methoxyphenyl)-4-oxo-1,3-thiazolidin-3-yl]propanamide **(15)**

Flash chromatography; CH_2Cl_2/EtOH, 98:2. Mp: 170°C (EtOH-H_2O), yield 43%. TLC; EtOAc/Hex, 1:1. FTIR (KBr, *v*, cm^{-1}): 3264 (NH), 3017-2933 (CH_3), 1721 (C=O), 1669 (CH=N). ^{1}H NMR (DMSO- d_6, δ, ppm): 10,61 (s, 1H, NH); 8,11 (d, 1H, *J*=8,0 Ar4); 7,72 (d, 1H, *J*=8,0 Ar7); 7,58 (t, 1H, *J*=7,6 Ar5); 7,30 (t, 1H, *J*=7,4 Ar6); 7,22 (d, 2H, *J*=8,4 Ar2'+6'); 6,88 (d, 2H, *J*=8,4 Ar3'+5'); 5,66 (s, 1H, CH); 4,27 (q, 1H, *J*=6,8 CH); 3,85 (d, 1H, *J*=16,0 CH-H); 3,79 (s, 3H, CH_3-O); 3,73 (d, 1H, *J*=16,0 CH-H); 1,54 (d, 3H, *J*=6,4 CH_3).

2-(1,2-Benzothiazol-3-yl)-N-[2-(4-fluorophenyl)-4-oxo-1,3-thiazolidin-3-yl]propanamide **(16)**

Mp: 185-186 °C (EtOH-H_2O), yield 87%. TLC; EtOAc/Hex, 1:1. FTIR (KBr, *v*, cm-1): 3230 (NH), 3031-2930 (CH_3), 1721 (C=O), 1665 (CH=N). ^{1}H NMR (DMSO- d_6, δ, ppm): 10,62 (s, 1H, NH); 8,160 (d, 1H, *J*=8,0 Ar2'+6'); 8,09 (d, 1H, *J*=8,0 Ar4); 7,74 (d, 1H, *J*=8,0 Ar7); 7,41 (t, 1H, *J*=7,8 Ar5); 7,31 (t, 1H, *J*=7,8 Ar6); 7,238-7,140 (m, 2H, Ar3'+5'); 5,73 (s, 1H, CH); 4,25 (q, 1H, *J*=7,2 CH); 3,89 (d, 1H, *J*=16,0 CH-H); 3,75 (d, 1H, *J*=16,0 CH-H); 1,54 (d, 3H, *J*=6,8 CH_3).

2-(1,2-Benzothiazol-3-yl)-N-{4-oxo-2-[4-(trifluoromethyl)phenyl]-1,3-thiazolidin-3-yl}propanamide **(17)**

Flash chromatography; CH_2Cl_2/MeOH(NH_3), 99:1. Mp: 145-147°C (EtOH-H_2O), yield 25%. TLC; EtOAc/Hex, 4:6. FTIR (KBr, *v*, cm^{-1}): 3220 (NH), 3028-2923 (CH_3), 1714 (C=O), 1663 (CH=N). ^{1}H NMR (DMSO- d_6, δ, ppm): 10,70 (s, 1H, NH); 8,15 (d, 1H, *J*=8,4 Ar4); 7,76-7,69 (m, 3H, Ar7+Ar3'+5'); 7,57-7,53 (m,3H, Ar5+Ar2'+6'); 7,20 (td, 1H, *J*=1,2 *J*=7,2 Ar6); 5,82 (s, 1H, CH); 4,29 (q, 1H, *J*=6,9 CH); 3,95 (dd, 1H, *J*=1,6 *J*=16,0 CH-H); 3,78 (d, 1H, *J*=15,60 CH-H); 1,54 (d, 3H, *J*=7,2 CH_3).

2-(1,2-Benzothiazol-3-yl)-N-[2-(4-chlorophenyl)-4-oxo-1,3-thiazolidin-3-yl]propanamide **(18)**

Mp: 187-188 °C (EtOH-H_2O), yield 97%. TLC; EtOAc/Hex, 1:1. FTIR (KBr, *v*, cm-1): 3219 (NH), 3029-2935 (CH3), 1718 (C=O), 1664 (CH=N). ^{1}H NMR (DMSO- d_6, δ, ppm): 10,65 (s, 1H, NH); 8,16 (d, 1H, *J*=8,0 Ar4); 7,74 (d, 1H, *J*=8,0 Ar7); 7,58 (t, 1H, *J*=7,6

Ar5); 7,39 (d, 2H, *J*=8,8 Ar33'+5') 7,32 (d, 2H, *J*=8,4 Ar2'+6'); 7,28 (t, 1H, *J*=7,6 Ar6); 5,73 (s, 1H, CH); 4,28 (q, 1H, *J*=7,2 CH); 3,90 (d, 1H, *J*=16,0 CH-H); 3,76 (d, 1H, *J*=16,0 CH-H); 1,54 (d, 3H, *J*=6,8 CH_3).

***2-(1,2-Benzothiazol-3-yl)*-N-*[2-(4-nitrophenyl)-4-oxo-1,3-thiazolidin-3-yl]propanamide* (19)**

Flash chromatography; CH_2Cl_2/EtOH (98:2). Mp: 208-209°C (EtOH-H_2O), yield 88%. TLC; EtOAc/Hex, 4:6. FTIR (KBr, *v*, cm^{-1}): 3247 (NH), 3030-2920 (CH_3), 1719 (C=O), 1664 (CH=N). ^{1}H NMR (DMSO- d_6, δ, ppm): 10,72 (s, 1H, NH); 8,14-8,12 (m, 3H, Ar4+Ar5+3'+5'); 7,76 (d, 1H, *J*=8,4 Ar7); 7,56 (d, 2H, *J*=8,4 Ar2'+6'); 7,52 (t, 1H, *J*=7,6 Ar5); 7,22 (t, 1H, *J*=7,6 Ar6); 5,88 (s, 1H, CH); 4,29 (q, 1H, *J*=7,0 CH); 3,95 (d, 1H, *J*=16,0 CH-H); 3,80 (d, 1H, *J*=16,0 CH-H); 1,51 (d, 3H, *J*=7,0 CH_3).

Synthesis of 3-{[2-(1,2-benzothiazol-3-yl)propanoyl]amino}-1,3-thiazolidin-4-ones 20-21

A mixture of the hydrazide **11** or **12** (1,1 mmol) and sulfanylacetic acid (2,2 mmol) was refluxed for 48 hours in 20 ml dry toluene, under a nitrogen atmosphere. After cooling to room temperature, the solvent was evaporated, and the oily residue was taken up with an aqueous solution of 10 % Na_2CO_3 and extracted (3×) with EtOAc. The organic phases were combined, dried (Na_2SO_4), and evaporated to afford a crude product which was purified by flash chromatography over silica gel (CH_2Cl_2/MeOH(NH_3), 99:1 as eluent) and recrystallized.

***4-(3-{[2-(1,2-Benzothiazol-3-yl)propanoyl]amino}-4-oxo-1,3-thiazolidin-2-yl)phenyl acetate* (20)**

Mp:120°C (EtOH-H_2O), yield 14%. TLC; CH_2Cl_2/EtOH, 95:5. FTIR (KBr, *v*, cm^{-1}): 3224 (NH), 3003-2935 (CH_3), 1747 (C=O), 1663 (CH=N). ^{1}H NMR (DMSO- d_6, δ, ppm): 10,73 (s, 1H, NH); 8,15 (d, 1H, *J*=8,4 Ar4); 7,69 (d, 1H, *J*=8,4 Ar7); 7,56 (t, 1H, *J*=7,2 Ar5); 7,37 (d, 2H, *J*=8,8 Ar2'+5'); 7,29 (t, 1H, *J*=7,2 Ar6); 7,14 (d, 2H, *J*=8,8 Ar2'+6'); 5,73 (s, 1H, CH); 4,28 (q, 1H, *J*=7,2 CH); 3,90 (dd, 1H, *J*=1,6 *J*=16,0 CH-H); 3,75 (d, 1H, *J*=15,60 CH-H); 2,31 (s, 3H, CH_3); 1,55 (d, 3H, *J*=7,2 CH_3).

***Methyl 4-(3-{[2-(1,2-benzothiazol-3-yl)propanoyl]amino}-4-oxo-1,3-thiazolidin-2-yl)benzoate* (21)**

Mp:144-145°C (EtOH-H_2O), yield 34%. TLC; CH_2Cl_2/EtOH, 95:5. FTIR (KBr, *v*, cm^{-1}): 3264 (NH), 3035-2917 (CH_3), 1708 (C=O), 1664 (CH=N). ^{1}H NMR (DMSO- d_6, δ, ppm): 10,71 (s, 1H, NH); 8,14 (d, 1H, *J*=8,4 Ar4); 7,88 (d, 2H, *J*=8,4 Ar3'+5'); 7,69 (d, 1H, *J*=8,1 Ar7); 7,54 (td, 1H, *J*=0,9 *J*=7,7 Ar5); 7,43 (d, 2H, *J*=8,4 Ar2'+6'); 7,19 (td, 1H, *J*=0,9 *J*=7,4 Ar6); 5,80 (s, 1H, CH); 4,27 (q, 1H, *J*=7,2 CH) 3,96-3,88 (m, 4H, CH-H + CH_3-O); 3,78 (d, 1H, *J*=15,6); 1,52 (d, 3H, *J*=6,9 CH_3).

Synthesis of target derivatives 22-23

To a stirred solution of the appropriate above 3-{[2-(1,2-benzothiazol-3-yl)propanoyl]amino}-1,3-thiazolidin-4-one **20** or **21**(0.6 mmol) in ethanol (30 mL) a 15% aqueous solution of NaOH (18 mL) was added and the resulting solution was stirred at room temperature for 2 hours. The ethanol was evaporated under reduced pressure, and then 1N HCl was added (to acidic pH), providing a white solid that was filtered off, washed with water and then recrystallised from ethanol-water.

***2-(1,2-Benzothiazol-3-yl)*-N-*[2-(4-hydroxyphenyl)-4-oxo-1,3-thiazolidin-3-yl]propanamide* (22)**

Mp: 257-259°C, yield 62%. TLC; CH_2Cl_2/EtOH, 95:5. FTIR (KBr, *v*, cm^{-1}): 3255 (NH), 2985-2935 (CH_3), 1721 (C=O), 1681 (CH=N). ^{1}H NMR (DMSO- d_6, δ, ppm): 10,58 (s, 1H, NH); 9,66 (s, 1H, OH); 8,16 (d, 1H, *J*=8,4 Ar4); 7,72 (d, 1H, *J*=8,0 Ar7); 7,59 (t, 1H, *J*=7,2 Ar5); 7,305 (t, 1H, *J*=7,2 Ar6); 7,12 (d, 2H, *J*=8,8 Ar2'+6'); 6,73 (d, 2H, *J*=8,4 Ar3+5'); 4,26 (q, 1H, *J*=6,8 CH); 3,82 (dd, 1H, *J*=1,2 *J*=15,0 CH-H); 3,71 (d, 1H, *J*=3,71 CH-H); 1,54 (d, 3H, *J*=6,4 CH_3).

***4-(3-{[2-(1,2-Benzothiazol-3-yl)propanoyl]amino}-4-oxo-1,3-thiazolidin-2-yl)benzoic acid* (23)**

Mp: 137-140°C, yield 90%. TLC; CH_2Cl_2/EtOH, 95:5. FTIR (KBr, *v*, cm^{-1}): 3248 (NH), 3005-2941 (CH_3), 1722 (C=O), 1667 (CH=N). ^{1}H NMR (DMSO- d_6, δ, ppm): 13,08 (s, 1H, COOH); 10,70 (s, 1H, NH); 8,14 (d, 1H, *J*=8,4 Ar4); 7,89 (d, 2H, *J*=8,4 Ar3'+5'); 7,70 (d, 1H, *J*=8,4 Ar7); 7,54 (t, 1H, *J*=7,4 Ar5); 7,43 (d, 2H, *J*=8,4 Ar2'+6'); 7,20 (t, 1H, *J*=7,4 Ar6); 5,79 (s, 1H, CH); 4,28 (q, 1H, *J*=7,2 CH); 4,28 (q, 1H, *J*=7,2 CH); 3,92 (dd, 1H, *J*=1,3 *J*=16,1 CH-H); 3,77 (d, 1H, *J*=16,00 CH-H); 1,54 (d, 3H, *J*=6,8 CH_3).

Preprints (www.preprints.org) | NOT PEER-REVIEWED | Posted: 31 October 2017 doi:10.20944/preprints201710.0200.v1

Peer-reviewed version available at Molecules 2018, 23, 415; doi:10.3390/molecules23020415

2.3. Biological evaluation

2.3.1. Antioxidant capacity

Free radicals and reactive oxygen species (ROS) are highly reactive molecules that are generated by normal cellular processes. They react with cellular components, damaging DNA, carbohydrates, proteins, and lipids and causing cellular and tissue injury. Moreover, an excess ROS production can lead to inflammation and several disease state, although organisms have developed complex antioxidant systems to protect themselves from oxidative substances. ORAC measures both lipophilic and hydrophilic antioxidant capacity and determines the ability of antioxidants to protect proteins from damage caused by free radicals [12]. ORAC assay has been widely accepted as a standard in vitro to measure the antioxidant activity of synthetic compounds, measuring their capacity to transfer hydrogen atom. The assay measures the loss of fluorescence over time due to peroxyl-radical formation by the breakdown of AAPH (2,2'-azobis-2- methyl-propanimidamide, dihydrochloride). Trolox [6-hydroxy-2,5,7,8-tetramethylchroman-2-carboxylic acid], a water soluble vitamin E analog, is a positive control that inhibits the fluorescein decay in a dose dependent manner. The ORAC assay is a kinetic assay measuring flurescein decay and antioxidant protection over time.

The tested 2-(1,2-benzothiazol-3-yl)-N-(4-oxo-2-phenyl-1,3-thiazolidin-3-yl)propanamides **(13-19, 22)** and the analogue **23** exhibited antioxidant activity, being able to delay the reduction of fluorescence of a fluorescein-AAPH solution appreciably (Table 1). In particular, compound **22** bearing a 4-hydroxyphenyl substituent at C2 of the 4-thiazolidinone ring showed excellent antioxidant effectiveness, producing appreciable effect than the reference Trolox (Table 1); the presence of a hydrophilic, electron donating and hydrogen bond forming group (OH) determines a greater activity than the analogues.

Table 1. Antioxidant activity of 4-thiazolidinones **13-19**, **22** and **23**

COMPOUNDS	R	ORAC UNIT [a]
13	-H	0.61 ± 0.14*
14	CH_3	0.40 ± 0.06*
15	$-OCH_3$	0.66 ± 0.12*
16	-F	0.46 ± 0.20*
17	$-CF_3$	0.27 ± 0.06*
18	-Cl	0.47 ± 0.23*

Preprints (www.preprints.org) | NOT PEER-REVIEWED | Posted: 31 October 2017 doi:10.20944/preprints201710.0200.v1

Peer-reviewed version available at Molecules 2018, 23, 415; doi:10.3390/molecules23020415

19	-NO_2	0.40 ± 0.17*
22	-OH	1.24 ± 0.09*
23	-COOH	0.53 ± 0.17*

[a]The ORAC values are reported as ORAC unit, corresponding to µmol of Trolox equivalents (TE) per micromol (µmol) of sample. Trolox = 1 ORAC Units. Reported values are the means±Standard deviation (SD) (n=3).
* Significantly different at $p<0.5$ compared to Trolox

2.3.2. Inhibitory activity on MMP-9

Matrix metalloproteases play crucial roles in many physiological or pathological events including tissue remodeling, ECM breakdown and the processing of a variety of biological molecules. MMP-9 is a Zn^{+2} dependent endopeptidase, synthesized and secreted in monomeric form as zymogen. Its primary function is degradation of proteins and particularly digests gelatin (denatured collagen), and types IV, V, XI and XVI collagen. Physiologically, MMP-9 in coordination with other MMPs, play a role in normal tissue remodeling events such as wound healing [13].

The synthesized compounds **13-19, 22** and **23** were tested for their *in vitro* ability to inhibit human recombinant MMP-9. Table 2 reports the results of this inhibition assay, expressed as IC_{50} (µM). Most of the tested compounds inhibited MMP-9, with IC_{50} values in the low micromolar range. We used as positive control a potent MMPs inhibitor, NNGH (N-isobutyl-N-(4-methoxyphenylsulfonyl)glycylhydroxamic acid) [14]. Compounds **22** and **23**, bearing hydrophilic and hydrogen bonds forming groups (OH and COOH), were the most active derivatives, with a IC_{50} value of 0.30 µM and 0.04 µM, respectively. Conversely the introduction, on the 4 position of the phenyl moiety at C2 of the 4-thiazolidinone ring, of a less hydrophilic group (OCH_3) or lipophilic methyl, nitro and halogens (Cl, F) substituents, led to 22 to 550 fold less potent MMP-9 inhibitors. Only the compound with the 4-trifluoromethylphenyl substituent at C2 of the 4-thiazolidinone ring did not show any inhibitory effectiveness toward MMP-9.

Table 2. *In vitro* inhibitory activity of 4-thiazolidinones **13-19**, **22** and **23** toward MMP-9

COMPOUNDS	R	IC_{50} value (µM)
13	-H	7.99 ± 0.65*

Preprints (www.preprints.org) | NOT PEER-REVIEWED | Posted: 31 October 2017 doi:10.20944/preprints201710.0200.v1

Peer-reviewed version available at Molecules 2018, 23, 415; doi:10.3390/molecules23020415

14	CH_3	9.01 ± 0.45*
15	$-OCH_3$	6.82 ± 0.95*
16	-F	17.15 ± 1.92*
17	$-CF_3$	n.a.
18	-Cl	16.12 ± 1.23*
19	$-NO_2$	22.05 ± 1.42*
22	-OH	0.30 ± 0.05*
23	-COOH	0.04± 0.01*
NNGH^		0.0065 ± 0.00025

n.a. = not active
^ NNGH ((N-Isobutyl-N-(4-methoxyphenylsulfonyl)glycylhydroxamic acid) is the reference standard of assay
Reported values are the means ± Standard Deviation (SD) (n = 3)
* $p<0.05$ compared to NNGH value

2.3.3. Cellular assay

In vitro biological activity of compounds **13-19, 22** and **23** was evaluated at different concentrations (100, 50 and 10 μM) using culture medium of human keratinocytes (NCTC 2544) stimulated for 48 h with 200 U/ml of IFN-γ and 10^{-4} M of histamine (H). All tested compounds reduce the ability of NCTC 2544 to metabolise tetrazolium salts at the doses of 100 and 50 μM, but not at 10 μM, demonstrating in this case that they did not interfere with cell viability (data not shown).

2.3.4. Determination of NF-κB levels

The inhibition of NF-kB expression, using Western blot analysis, was evaluated on compounds **22** and **23**, the 4-thiazolidinones derivatives which possess the most potent inhibitory effect against MMP-9 and antioxidant activity (Figure 2).

The treatment of keratinocyte cell line NCTC 2544) with 200 U/ml of IFN-γ and 10^{-4} M of histamine (H) increased NF-kB levels compared to untreated cells. IFN-γ is an essential cytokine in amplifying inflammatory reactions, as it stimulates the synthesis of chemokines that attract inflammatory cells and induces expression of molecules important for the retention and activation of T cells. We employed both IFN-γ and histamine because they use distinct signal transduction pathways, and this can lead to a stronger activation of inflammatory genes. Histamine is released from mast cells and keratinocytes in the early

stage of inflammation of the skin and participates in the control of the inflammatory responses by acting on lymphocytes, monocytes, and leukocytes. Histamine binds to cell surface receptors coupling to guanine nucleotide-binding protein (G-protein) and induces various intracellular signalling pathways. These histamine-receptor-mediated signals regulate cytokine or chemokine gene expression in target cells [15]. Stimulated keratinocytes were treated with compounds **22** and **23** and the levels of NF-kB were measured after 48 hours. All compounds reduced NF-kB release at 10 μM concentrations. The best results were obtained with **23** which provided up to 50% reduction of NF-kB levels compared to IFN-γ and H-treated cells.

The observed ability of compounds **22** and **23** to reduce NF-kB levels in keratinocytes appears to be of interest since this is an upstream event. Infact the NF-kB reduction can lead to decreased levels of other pro-inflammatory mediators, such as cytokines and different enzymes (such as MMPs, iNOS), interfering with downstream signaling components crucial for inflammatory response and degenerative processes involved in arthritis.

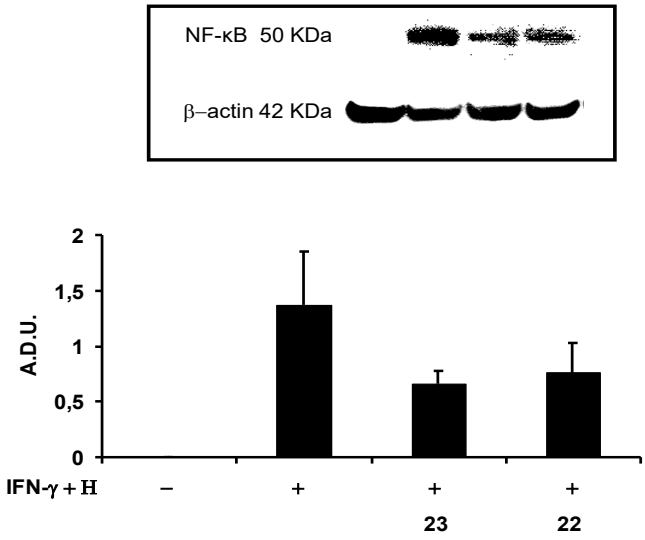

Figure 2. Effects of **22** and **23** on NF-κB expression. (a) Representative blot. (b) Nuclear Factor-kappa B (NF-κB) levels in cultures of human keratinocytes stimulated with IFN-γ and histamine (H), 48 h after the addition of compounds **22** and **23** at 10 □M concentrations, determined by Western blot analysis. Data show the relative expression (mean ± SEM) of NF-kB, calculated as arbitrary densitometric units (A.D.U.), from three independent experiments. P <0.05, compared with respective IFN-γ and H.

2.3.5. Docking studies on MMP-9

To rationalize the observed activity data, all syntetized compounds were docked into the active site of MMP-9 using the software Accelrys Discovery Studio 3.5 [16]. MMP inhibitors generally follow a two-component strategy, which is designed to interact in a noncovalent fashion with the MMP active site, while an appended zinc(II)-chelating moiety binds via coordinate–covalent bonds to the hydrolytic zinc(II) ion, rendering the enzyme inactive [17,18]. According to ZBG studies, using the coordinates of protein-ligand complex structures obtained from the PDB, the most frequently found ZBG is carboxylate, followed by sulfonamide, hydroxamate, and phosphonate/phosphate. Whereas carboxylates bound to the zinc via both monodentate and bidentate interactions, the hydroxamates bound dominantly in a bidentate manner [19]. The median distances from the nitrogen, oxygen, and sulfur atoms were 1.99, 2.05, and 2.28 Å respectively. The median distance from sulfur was the longest among these three heteroatoms. The differences among these distances were thought to be the result of the different sizes of the elements [20].

The catalytic centre of MMP-9 is composed of the active-site zinc ion, coordinated by three histidine residues (His401, His405 and His411) and the essential glutamic acid residue (Glu402). The crystal structure of the MMP-9, complexed with a reverse hydroxamate inhibitor (NFH), was retrieved from the Protein Data Bank (PDB ID: 1GKC) [21]. According to the docking results, NFH showed hydrogen bonds with Gly186, Leu188, Tyr421 (water mediated), Tyr423 and a π–sigma interaction with His401; these are in accordance with the X-ray structure binding features [21]. The reference drug NNGH showed hydrogen bonds with Leu188, Ala189, Glu402 and a π–π interaction with His401. The most potent MMP-9 inhibitor, compound **23**, which has carboxylate group as an ZBG, revealed hydrogen bonds with Gly186, Tyr423 and His401 (Figure 3c). The van der Waals contact distances between the oxygen atoms of NFH and Zn atom are 2.04 and 1.956 Å (Figure 3b). The van der Waals contact distances between the oxygen atoms of NNGH and Zn atom are 2.38 and 2.92 Å. Similarly, the van der Waals contact distance between the carboxylate oxygen of compound **23** and Zn atom is 1.978 Å (Figure 3c). Among all tested compounds **23** has the only carboxylate group on R position. According to docking results carboxylate group of **23** has a monodentate interaction with Zn atom, so this could be explain it's higher activity. When we look at the moderately active compound **22**, it showed hydrogen bonds with Gly186, Ala189 and the van der Waals contact distance between the

Preprints (www.preprints.org) | NOT PEER-REVIEWED | Posted: 31 October 2017 doi:10.20944/preprints201710.0200.v1

Peer-reviewed version available at Molecules 2018, 23, 415; doi:10.3390/molecules23020415

carbonyl oxygen atom of amide function of **22** and Zn atom is 1.715 Å (Figure 3d). Compounds **17** and **18** have interactions with Zn atom similar to **22**. But both of them have only one hydrogen bond (water mediated) with the enzyme. Although they have interactions with Zn atom their activities are lower, because of the weak interaction with the enzyme MMP-9. Docking results of the other lower active compounds (**13**, **14**, **15**, **16, 19**) showed H bonds with some of the active site residues but none of them has interaction with Zn atom. All of the docking results are given in Table 3.

Table 3. Interacted residues of the tested compounds according to the docking results

Compound	Interacted Residues*
13	Gly186, Leu187, **Leu188** (1.66 Å), Ala189, His190, Ala191, Tyr393, Val398, His401, **Glu402** (2.40 Å), His405, His411, Pro421, Met422, **Tyr423** (1.89 Å)
14	Gly186, Leu187, **Leu188**[b] (1.92 Å), Ala189, Tyr393, Leu397, Val398, His401[a], Glu402, Leu418, Tyr420, **Pro421** (2.30 Å), Met422, Tyr423, Arg424
15	Gly186, Leu187, **Leu188** (2.19 Å), **Ala189** (2.13 Å), His190, Tyr393, Leu397, Val398, His401[a], Glu402, Leu418, Tyr420, Pro421, Met422, **Tyr423** (2.28 Å), Arg424
16	Gly186, Leu187, **Leu188** (1.73 Å), Ala189 (2.18 Å), His190, Ala191, Tyr393, Val398, His401, **Glu402** (2.44), His405, Pro421, Met422, **Tyr423** (1.48 Å)
17	Phe110, Glu111, Leu187, Leu188, Ala189, His190, **Ala191** (2.49 Å) (water mediated), Val398, His401[a], Glu402, His405, His411, Tyr420, Pro421, Met422, Tyr423, Zn
18	Phe110, Glu111, Gly186, Leu187, Leu188, Ala189, His190, **Ala191** (2.37 Å) (water mediated) His401, Glu402, His405, His411, Pro421, Met422, Tyr423, Zn
19	Gly186, Leu187, Leu188, **Ala189** (2.24 Å), His190, Val398, His401, Glu402, His405, His411, Pro421, Met422, Tyr423
22	Phe110, Glu111, **Gly186** (1.75 Å), Leu187, Leu188, **Ala189** (2.12 Å), His190, Ala191, Val398, His401, Glu402, His405, His411, Pro421, Met422, Tyr423, Zn

Preprints (www.preprints.org) | NOT PEER-REVIEWED | Posted: 31 October 2017 doi:10.20944/preprints201710.0200.v1

Peer-reviewed version available at Molecules 2018, 23, 415; doi:10.3390/molecules23020415

23	Asp185, **Gly186** (2.03 Å), Leu187, Leu188, Tyr393, **His401** (2.26 Å), Glu402, His411, Pro421, Met422, **Tyr423** (2.35 Å), Zn
NFH	**Gly186** (2.32), Leu187, **Leu188** (1.92 Å), Ala189, His190, Ala191, Tyr393, Val398, His401[b], Glu402, His405, His411, Tyr420, **Pro421** (2.04 Å) (water mediated), Met422, **Tyr423** (2.15 Å), Zn
NNGH	Gly186, Leu187, **Leu188** (2.17 Å), **Ala189** (2.19 Å), His190, Ala191, Leu397, Val398, His401[a], **Glu402** (1.34 Å), His405, His411, Leu418, Tyr420, Pro421, Met422, Tyr423, Arg424, Zn

Bold: H-bonds, [a]: π-π interactions, [b]: π-sigma interactions
* van der Waals contact distance <4 Å

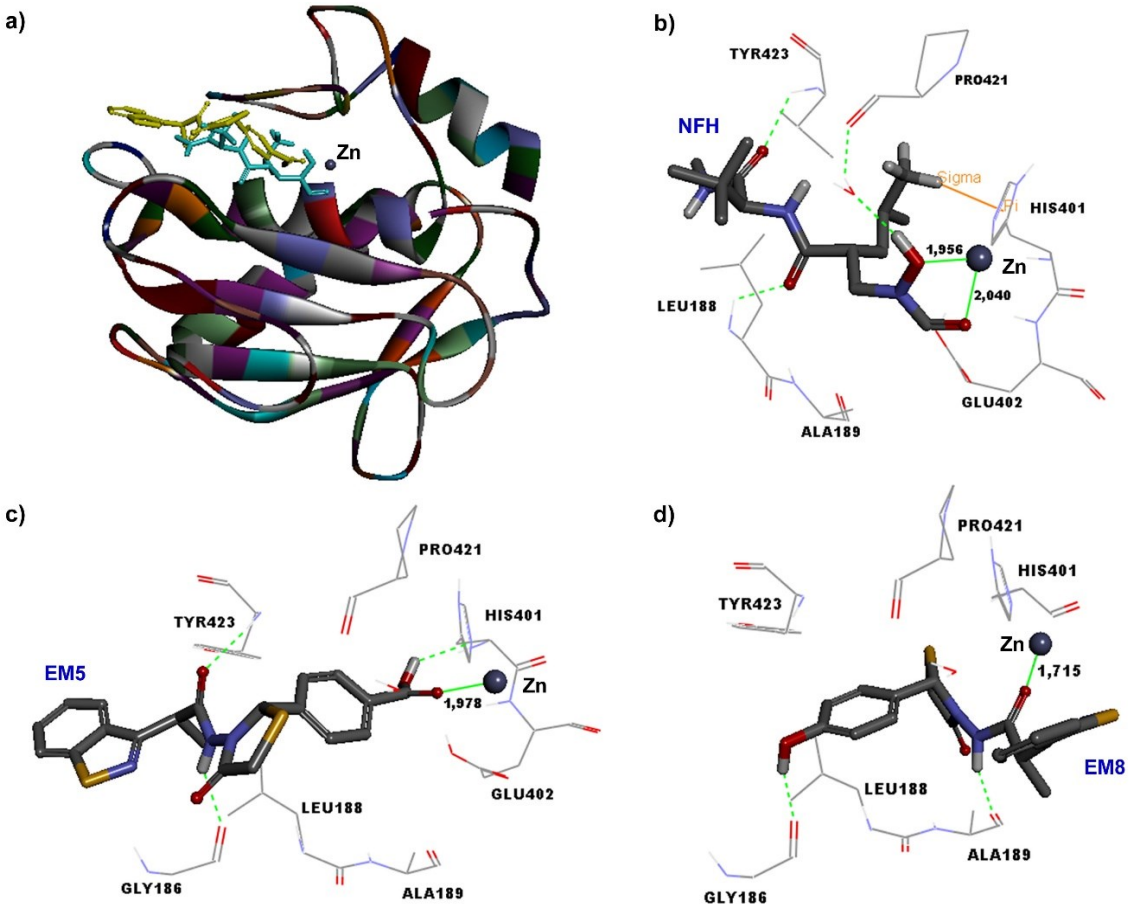

Preprints (www.preprints.org) | NOT PEER-REVIEWED | Posted: 31 October 2017 doi:10.20944/preprints201710.0200.v1

Peer-reviewed version available at Molecules 2018, 23, 415; doi:10.3390/molecules23020415

Figure 3. a) Binding modes of **23** (yellow) and NFH (blue). **b)** Docking position* of NFH: showed hydrogen bonds with Gly186, Leu188, Tyr421(water mediated), Tyr423 and a π–sigma interaction with His401. **c)** Docking position* of **23**: showed hydrogen bonds with Gln186, Tyr423 and His401. **d)** Docking position* of **22**: showed hydrogen bonds with Gln186, Ala189.
* All hydrogen bonds are shown as green dashed lines and all distances are shown as green lines

3. Materials and Methods

All chemicals were from Sigma Aldrich Co (St. Louis, USA).

3.1. Oxygen radical absorbance capacity (ORAC) assays

The ORAC assay was performed as previously reported by Cao et al. [22]. The measurements were carried out on a Wallac 1420 Victor^3 96-well plate reader (EG & Wallac, Turku, Finland) with fluorescence filter (excitation 540 nm/8 nm, emission 570 nm/7 nm). Fluorescein (10 nM) was the fluorescence probe and target molecule for free radical attack from AAPH (100 mM) as peroxyl radical generator. The reaction was conducted at 37 °C at pH 7.0 with Trolox (12,5 μM) as control standard and phosphate buffer as blank. Compounds **13-19** and **22-23** were appropriately diluted with DMSO/buffer (1: 10) prior to analysis. The fluorescein fluorescence was recorded every 2 min after addition of AAPH. All measurements were expressed relative to the initial reading. One blank, one standard, and a maximum of 10 samples were analyzed at the same time. Each measure was repeated at least three times. The ORAC value refers to the net protection area under the quenching curve of fluorescein in the presence of an antioxidant. The final results (ORAC value) were calculated and expressed using Trolox equivalents (TE) per gram of extract (TE/g)

$$\text{ORAC value } (\mu M) = K(S \text{ sample} - S \text{ blank})/(S \text{ Trolox} - S \text{ blank})$$

Where K is a sample dilution factor, S is the area under the fluorescence decay curve of the sample, Trolox or blank. This area was calculated with Origin®7 (OriginLab Corporation, Northampton, USA).

3.2. MMP-9 fluorimetric assay

The compounds were evaluated for their ability to inhibit the hydrolysis of fluorescence-quenched peptide substrate Mca-Pro-Leu-Gly-Leu-Dpa-Ala-Arg-NH_2 (Biomol, Inc.). The MMP-9 assays were performed in 50 mM HEPES buffer containing 5 mM $CaCl_2$, 0.1 mM

$ZnCl_2$, 0.05% Brij-35, at pH 7, using 10 nM of proteolytic enzyme (catalytic domains of MMP-9 (Biomol, Inc.) and 350 nM of peptide substrate.

The enzyme was incubated at 25°C with increasing concentration of the inhibitor and the fluorescence (excitation $_{max}$ 328 nm; emission $_{max}$ 393 nm) was measured for 3 min after the addition of the substrate using a Varian Eclipse fluorimeter. Fitting of rates as a function of inhibitor concentration provided IC_{50} values. The inhibitor N-isobutyl-N-[4-methoxyphenylsulfonyl]glycyl hydroxamic acid (Biomol, Inc.) was used as control [23].

3.3. Keratinocyte cultures and treatments

The normal human keratinocyte cell line NCTC 2544 was provided by Interlab Cell Line Collection Genoa, Italy) and cultured in Minimum Essential Medium (MEM) (Sigma-Aldrich, Milan, Italy) containing 10% fetal calf serum, 100 U/ml penicillin and 100 µg/ml streptomycin at 37 °C in a humidified, 95% air/5% CO_2 atmosphere. The medium was changed every 2–3 days. A day before the experiment, cells were trypsinized, counted, and plated either in 96 wells or in 6 well plates. Experimental keratinocytes were stimulated or not (untreated controls) with 200 U/ml of IFN-γ and 10^{-4} M of histamine (H) in presence or absence of different concentrations of EM compounds (10, 50 and 100 µM). After 48 hours each sample was tested for the experiments described below.

3.4. Cell viability assay

The cytotoxic effect of the experimental substances was evaluated by a cell viability test based on the cleavage of 3-(4,5-dimethylthiazol-2-yl)-2,5-diphenyltetrazolium bromide (MTT) by mitochondrial dehydrogenases of metabolically active cells [24].

3.5. Western blot analysis

The expression of nuclear factor kappa-light-chain-enhancer of activated B cells (NF-kB)□ was evaluated by Western blot analysis. Treated and untreated cells were trypsinized, pelletted and washed three times with PBS. Proteins were extracted by M-PER® Mammalian Protein Extraction Reagent (Thermo scientific, Pierce Biotechnology) supplemented with a cocktail of protease inhibitors (complete, Mini, Protease Inhibitor Cocktail Tablets, Roche) according to manufacturer's instructions and the protein concentration was estimated using the Bicinchoninic acid assay (Pierce). Equal amount of proteins was boiled in LDS sample buffer (Invitrogen) in presence of 1X sample reducing

agent (Invitrogen). Each sample was then subjected to electrophoresis on Bolt™ 4-12% Bis-Tris Plus Gels (Invitrogen). After electrophoresis, proteins were transferred to nitrocellulose membrane, in a wet system, and proteins transfer was verified by staining membranes with Ponceau S. Membranes were blocked with Tris buffered saline containing 0.01% Tween-20 (TBST) and 5% non-fat dry milk for 1 hour RT, and then probed overnight at 4 °C with the following primary antibodies: anti- NF-κB p-50 and anti- β-actin. The membranes were rinsed three times in TBST and the appropriate HRP-conjugated secondary antibody was incubated for 1 hour at RT. The blots were developed using enhanced chemiluminescent solution (Millipore) and visualized with a chemiluminescent western blot imaging systems (Alliance, UVITEC). Bands were measured densitometrically and their relative density was calculated based on the density of the β-actin in each sample. Results were expressed as arbitrary densitometric units (A.D.U.) corresponding to signal intensity with respect to loading control.

3.6. Statistical analysis

All the present results are means S.E.M. of three experiments performed on quadruplicate samples. The Student's t-test was used to evaluate the differences between the means of each group. $P < 0.05$ was considered to be statistically significant. The statistical analysis was performed by using one-way ANOVA followed by Dunnett's post-hoc test for multiple comparison with control. All statistical analyses were performed using the statistical software package SYSTAT, version 9 (Systat Inc., Evanston IL, USA).

3.7. Docking studies

3.7.1. Preparation of the Enzyme

The crystal structure of the MMP-9, complexed with a reverse hydroxamate inhibitor (NFH) was retrieved from the Protein Data Bank (PDB ID: 1GKC) [21]. Accelrys Discovery Studio 3.5 [16] software was used for preparation of protein and ligands. The target protein was taken, the ligand was extracted, hydrogens were added and their positions were optimized using the all atom CHARMm forcefield and the Adopted Basis set Newton Raphson (ABNR) method available in Discovery Studio 3.5 protocol until the root mean deviation (RMS) gradient was < 0.05 kcal / mol / $Å^2$. The minimized protein was defined as the receptor using the binding site module. The binding site was defined from the cavity

Preprints (www.preprints.org) | NOT PEER-REVIEWED | Posted: 31 October 2017 doi:10.20944/preprints201710.0200.v1

Peer-reviewed version available at Molecules 2018, 23, 415; doi:10.3390/molecules23020415

finding method which was modified to accommodate all the important interacting residues in the active site. Binding sphere for 1GKC (65.86, 30.94, 118.05, 9.78) was selected from the active site using the binding site tools.

3.7.2. Preparation of Ligands

Novel synthesized 4-thiazolidinone derivatives **13-19** and **22-23**, NFH and standard drug NNGH were sketched, all atom CHARMm forcefield parameterization was assigned and then minimized using the ABNR method as described above. Conformational searches of the ligands were carried out using a simulated annealing molecular dynamics (MD) approach. The ligands were heated to a temperature of 700 K and then annealed to 200 K.

3.7.3. Molecular Docking

CDocker [25] method was performed by using Discovery Studio 3.5. The protein is held rigid while the ligands are allowed to be flexible during refinement. The docking parameters were as follows: Top Hits: 10; Random Conformations: 10; Random Conformations Dynamics Step: 1000; Grid Extension: 8.0; Random Dynamics Time Step: 0.002. The docking and scoring methodology was first validated by docking of NFH. The docked position of NFH overlaps well with the crystal structure position, with an RMSD of 0.29 Å. Afterwards molecular docking studies were performed on the new synthesized compounds.

3.7.4. Analysis of Results

Finally, all docked poses were scored by applying Analyze Ligand Poses subprotocol and binding energies were calculated by applying Calculate Binding Energy subprotocol in Discovery Studio 3.5 by using in situ ligand minimization step (ABNR method) and using implicit solvent model (GBMV). The lowest binding energy was taken as the best-docked conformation of the compound for the macromolecule.

4. Conclusions

On the whole our results indicate that the appreciable anti-inflammatory/wound healing effects of the compounds tested are supported by the 4-thiazolidinone core, the benzisothiazole system and the isopropanoylhydrazide spacer, whereas the 4-phenyl substituent at C2 of the 4-thiazolidinone ring appears to be able to modulate their activity. Among the tested compounds derivative **23**, bearing a 4-carboxyphenyl substituent at C2 of

the 4-thiazolidinone ring, exhibited the most promising profile, being able to inhibit MMP-9 at nanomolar level (IC_{50} = 40 nM) and to reduce NF-kB levels (50% at 10 µM.). Accordingly, **23** shows good antioxidant activity (ORAC value = 0,53 TE/ µmol). Docking studies, performed as reported above, show that carboxylate group of 23 has a monodentate interaction with Zn atom and H bonds with three of the active site residues (Gly186, Tyr423 and His401) that could explain its higher activity. 4-(3-{[2-(1,2-Benzothiazol-3-yl)propanoyl]amino}-4-oxo-1,3-thiazolidin-2-yl)benzoic acid **23** can therefore be considered as a lead compound for the development of new therapeutic agents to prevent tissue damage.

References

1. Simopoulos, A.P.; Milner, J. 3rd Congress of the International Society of Nutrigenetics/Nutrigenomics (ISSN) Bethesda, Maryland, USA, 21-23 October. *J. Nutrigenet. Nutrige* 2009, *2,* 189–224, DOI: 10.1159/000281017.

2. Crascì, L.; Lauro, M.R.; Puglisi,G.; Panico, A.M. Natural Antioxidant Polyphenols On Inflammation Management: Anti-glycation Activity Vs Metalloproteinases Inhibition. *Crit Rev Food Sci*. 2016**,** 00-00, DOI:10.1080/10408398.2016.1229657.

3. Baker, R.G.; Hayden, M.S.; Ghosh, S. NF-κB, inflammation, and metabolic disease. *Cell. metab*. 2011, *13*(1), 11-22, DOI:10.1016/j.cmet.2010.12.008.

4. Hsieh, H.L.; Yang, C.M. Role of redox signaling in neuroinflammation and neurodegenerative diseases. *BioMed. Res-Int.* 2013, DOI:10.1155/2013/484613.

5. Hu, J.; Van den Steen, P.E.; Sang, Q.X.A.; Opdenakker, G. Matrix metalloproteinase inhibitors as therapy for inflammatory and vascular diseases. *Nat. Rev. Drug Discov.* 2007, 6(6), 480-498, DOI:10.1038/nrd2308.

6. Tallant, C.; Marrero, A.; Gomis-Rüth, F.X. Matrix metalloproteinases: fold and function of their catalytic domains. *BBA. Molecular cell. research.* 2010, 1803(1), 20-28, DOI:10.1016/j.bbamcr.2009.04.003.

7. Gupta, S.P. Quantitative structure-activity relationship studies on zinc-containing metalloproteinase inhibitors. *Chem. Rev*. 2007,*107*(7), 3042-3087, DOI:10.1021/cr030448t.

8. Bordi, F.; Mor, M.; Plazzi, P. V.; Silva, C.; Morini, G.; Impicciatore, M.; Barocelli, E.; Chiavarini, M. 4-(1,2-benzisothiazol-3yl-)alkanoic and phenylalcanoic acids: synthesis and anti-inflammatory, analgesic and antipyretic activities. IL Farmaco (1992), 47(5), 551-65.

9. Vitali, T.; Lugari Mangia, M.T. Cytotoxic activity of 2-methyl-2(1,2-benzisothiazol-3-yl) acetic acid derivatives. Ateneo Parmense, *Acta Nat.* 1973, 9(1), 29-37.

10. Giméneza, R.; Oriola, L.; Piñolb, M.; Serrano, J. L.; Viñualesa, A. I.; Fisherc, T.; Stumpe, J. Synthesis and Properties of 2-Phenylbenzoxazole-Based Luminophores for in situ Photopolymerized Liquid-Crystal Films Helvetica. *Acta Chim. 2006,* 89, 304-319, DOI:10.1002/HLCA.200690035.

11. Kato, T.; Saito, N.; Kashimura, K.; Shinohara, M.; Kurahashi, T.; Taniguchi, K. Germination and Growth Inhibitors from Wheat (Triticum aestivum L.) Husks. *J. Agric. Food Chem.* 2002, 50, 6307−6312, DOI:10.1021/jf0204755.

12. Prior, R.L.; Wu, X.; Schaich, K. Standardized methods for the determination of antioxidant capacity and phenolics in foods and dietary supplements. *J. Agric. Food Chem. 2005, 53*(10), 4290-4302, DOI:10.1021/jf0502698.

13. Kampoli, A.M.; Tousoulis, D.; Papageorgiou, N.; Antoniades, C.; Androulakis, E.; Tsiamis, E.; Stefanadis, C. Matrix metalloproteinases in acute coronary syndromes: current perspectives. *Curr. Top. Med. Chem. 2012,12*(10), 1192-1205.

14. Calderone, V.; Fragai, M.; Luchinat, C.; Nativi, C.; Richichi, B.; Roelens, S. A High - Affinity Carbohydrate - Containing Inhibitor of Matrix Metalloproteinases. *Chem. Med. Chem*. 2006, *1*(6), 598-601, DOI:10.1002/cmdc.200600020.

15. Cardile, V.; Libra, M.; Caggia, S.; Frasca, G.; Umezawa, K.; Stivala, F.; Mazzarino, M.C.; Bevelacqua, Y.; Coco, M.; Malaponte, G. Dehydroxymethylepoxyquinomicin, a novel nuclear factor-kappaB inhibitor, prevents inflammatory injury induced by interferon-gamma and histamine in NCTC 2544 keratinocytes. *Clin. Exp. Pharmacol. P.* 2010, 37(7), 679-83,DOI:10.1111/j.1440-1681.2010.05375.x.

16. Discovery Studio 3.5. *Accelrys Inc.* 2012.

17. Whittaker, M.; Floyd, C.D.; Brown, P.; Gearing, A. J. Design and therapeutic application of matrix metalloproteinase inhibitors. *Chem. Rev*. 1999, *99*(9), 2735-2776. DOI:10.1021/cr9804543.

18. Puerta, D.T.; Cohen, S.M. A bioinorganic perspective on matrix metalloproteinase inhibition. *Curr Top Med Chem. 2004, 4*(15), 1551-1573, DOI:10.2174/1568026043387368.

19. Kawai, K.; Nagata, N. Metaleligand interactions: An analysis of zinc binding groups using the Protein Data Bank. *Med. Chem. Eur. J. 2012,* 51, 271-276, DOI:10.1016/j.ejmech.2012.02.028.

20. Harding, M.M. Geometry of metal-ligand interactions in proteins. *Acta Crystallogr. D. 2001,* 57, 401-411, DOI:10.1107/S0907444900019168.

21. Rowsel,l S.; Hawtin, P.; Minshull, C.A.; Jepson, H.; Brockbank, S.M.V.; Barratt, D.G.; Slater, A.M.; McPheat, W.L.; Waterson, D.; Henneyand, A.M.; Pauptit, R.A. Crystal Structure of Human MMP-9 in Complex with a Reverse Hydroxamate Inhibitor. *J. Mol. Biol.* 2002, *319,* 173–181; DOI:10.1016/S0022-2836(02)00262-0.

22. Cao, G.; Alessio, H.M.; Cutler, R.G. Oxygen-radical absorbance capacity assay for antioxidants. *Free radical Bio Med*. 1993, *14*(3), 303-311, DOI:10.1016/0891-5849(93)90027-R.

23. Crascì, L.; Vicini, P.; Incerti, M.; Cardile, V.; Avondo, S.; Panico, A. 2-Benzisothiazolylimino-5-benzylidene-4-thiazolidinones as protective agents against cartilage destruction. *Bioorgan. Med. Chem. 2015, 23*(7), 1551-1556, DOI:10.1016/j.bmc.2015.02.002.

24. Panico, A.M.; Vicini, P.; Massimo, G.; Cardile, V.; Gentile, B.; Avondo, S.; Vittorio, F.; Ronsisvalle, G. Protective effects of benzisothiazolylamidines on IL-1β induced alterations in human articular chondrocyte metabolism. *Inflammation 2004*, 28(4), 231-235, DOI: 10.1023/B.

25. Wu, G.; Robertson, D.H.; Brooks, C.L.; Vieth, M. Detailed analysis of grid-based molecular docking: A case study of CDOCKER—A CHARMm-based MD docking algorithm. *J. Comput Chem*. 2003, *24*(13), 1549-1562; DOI:10.1002/jcc.10306.